AJAB

Asian J Agric & Biol. xxxx(x).
DOI: 10.35495/ajab.2023.245

Original Article

Green synthesis of zinc oxide microparticles using the leaf extract of *Dolichandrone spathacea* in sustainable agriculture: a new approach for protecting the legume plant (*Vigna radiata*) against the Cr(VI) stress

Nguyen-Huan Pham-Khanh[1], Nhat-Quynh Huynh[1], Hong-Ngoc-Bao Le[1], Thi-Kim-Quy Ha[1*]
[1]College of Natural Sciences, Can Tho University, Campus II, 3/2 street, Ninh Kieu district, Can Tho City 94000, Vietnam

Received:
October 06, 2023
Accepted:
January08, 2024
Published Online:
February 15, 2024

**Corresponding author email:*
htkquy@ctu.edu.vn

Abstract

The hazardous heavy metal ion Cr(VI) is harmful and easily mobile in the environment. Cr(VI) poisoning can cause delayed seed germination and damaged plant growth. This study suggested a green and simple synthesis method of ZnO microparticles (ZnO MPs) from $Zn(CH_3COO)_2$ solution and aqueous leaf extract of *Dolichandrone spathacea* (L. f.) K. Schum for protecting the legume plant (*Vigna radiata*) against the Cr(VI) stress. The optimized conditions for the synthesis of these MPs were determined using computational and experimental approaches. The characterization of ZnO MPs was analyzed by surface morphology, particle sizes, and elemental components using modern methods. The Zn MPs successfully exhibited the potential protective effects on the seed germination and seedling vigor of *V. radiata* under Cr(VI) stress. The results of PPR and ABTS assays also indicated that the antioxidant capacity of non-enzymatic antioxidants from leaves under Cr(VI) stress significantly reduced (46.83 ± 1.938% and 69.60 ± 2.17%, respectively) as compared to supplement of ZnO-MPs increased (55.44 ± 2.624% and 78.07 ± 0.820%, respectively). This study is an essential report for the agricultural field, which can apply further the new and green zinc-micronutrient fertilizer to mitigate the adverse effects of heavy metal contamination on crop cultivation.

Keywords: Green synthesis, Zinc oxide microparticles, *Dolichandrone spathacea*, Cr(VI) stress, *Vigna radiata*.

How to cite this:

Pham-Khanh NH, Huynh NQ, Le HNB and Ha TKQ. Green synthesis of zinc oxide microparticles using the leaf extract of *Dolichandrone spathacea* in sustainable agriculture: a new approach for protecting the legume plant (*Vigna radiata*) against the Cr(VI) stress. Asian J. Agric. Biol. xxxx(x): 2023245. DOI: https://doi.org/10.35495/ajab.2023.245

Introduction

In recent decades, the development of industry and the rising population have led to the release of various heavy metals into the environment, creating a risk to both human health and ecological systems. Chromium (Cr) is one such heavy metal that is widely present and highly toxic in wastewater and soil (Choppala et al., 2013). In aqueous systems, Cr can exist in two forms - trivalent and hexavalent

oxidation states, both of which have different levels of toxicity. Trace amounts of Cr(III) are relatively safe and even essential for plant growth in regulating glucose metabolism (Ali et al., 2023). Cr(VI) is highly toxic as it is easily mobile in the environment and can cause cancer in living organisms (Karimi-Maleh et al., 2021). Plants can exhibit signs of toxicity from Cr(VI), such as delayed seed germination, damaged roots with decreased development, decreased biomass, reduced plant height, impaired photosynthesis, leaf chlorosis, low grain production, and, ultimately, plant death. The hindering of mitochondrial electron transport in Tracheophyta by Cr leads to the increase in the production of reactive oxygen species and oxidative stress, as well as changing to pigments and chloroplasts (Hauschild, 1993). Many studies have focused on using microorganisms or chemical reagents to reduce the toxicity of Cr(VI) using various types of plants for experiment setups, such as *Triticum aestivum*, *Oryza sativa* L. Damini, *Zea mays* L., and *Vigna radiata*, resulting in a reduction in root length, biomass, gene regulation, and oxidative responses (Arshad et al., 2017; Cheung and Gu, 2007; Prakash et al., 2022; Ramzan et al., 2023; Singh et al., 2021). However, the published processes for the synthesis of materials are usually complex and challenging to access for farmers in developing countries. Therefore, it is currently necessary to propose a simple method for synthesizing environmentally benign materials that can protect plants from hazardous agents of Cr(VI).

Nanotechnology and microtechnology have advanced significantly in various fields that benefit human welfare (Sun et al., 2020). One of its recent applications involves the synthesis of ZnO nanoparticles (ZnO NPs) and microparticles (ZnO MPs) for use in biomedical, environmental treatment, and catalytic applications (Jin and Jin, 2021; Saffari et al., 2020). Recently, many methods were published for the synthesis of ZnO NPs, which commonly required a calcination step and used a muffle furnace, which required more energy, resources, and complex processes (Abdelbaky et al., 2022; Karam and Abdulrahman, 2022). A more sustainable, low-energy synthesis method is necessary, particularly for developing countries. Based on our knowledge, there has been no published research on the potential application of aqueous extract from *Dolichandrone spathacea* (L. f.) K. Schum for synthesizing ZnO MPs, and not many studies have investigated the simplest method to create the ZnO MPs but still protect plants against Cr(VI) toxins.

Dolichandrone spathacea (L. f.) K. Schum belongs to the Bignoniaceae family which is found in mangrove forests along the coastal regions in some Southeast Asian countries. *D. spathacea* has been used as a traditional medicinal for liver detoxification, antitumor treatment, antiseptic use, and treatment of nervous diseases (Thao et al., 2021). *D. spathacea* contains several types of secondary metabolites, such as iridoids, phenolics, saponins, triterpenoids, and steroids, that have significant biological effects (Nguyen et al., 2018). These metabolites could be used as potential reagents for the green synthesis of ZnO MPs.

Mungbean (*Vigna radiata*), a crop widely cultivated in Asia, is ranked third in importance among pulse crops, trailing only chickpea and pigeon peas (Nair et al., 2019). It is a short-duration crop, typically grown under rainfed conditions, and is highly versatile and suitable for catch cropping, intercropping, relay cropping, and soil nutrient enhancement. This plant is often grown in hot climates and marginal lands, making it moderately drought-tolerant. This characteristic makes it a valuable crop for studying how it tolerates different types of stress (Kim et al., 2015). Recently, it was reported that ZnO particles could affect the growth of mungbean (Jayarambabu et al., 2015; Rani et al., 2023), but it is not yet known how ZnO MPs would affect mungbean under Cr(VI) toxicity at different growth stages, such as seed germination and seedling vigor stages.

In this study, green methodology to synthesize ZnO MPs using the leaf extract of *D. spathacea* without the calcination step and the developed response surface method (RSM) model were performed to estimate the suitable conditions between the computational and experimental design. These particles were evaluated for their ability to protect legume plants against oxidative stress by Cr(VI) toxins.

Material and Methods

Plant materials and extraction

The leaves of *D. spathacea* were collected in Dong Hai district, Bac Lieu province, Vietnam, and botanically authenticated by Dr. Pham Ha Thanh Tung, Phenikaa University, Vietnam. Two kg of leaves were washed with tap water to remove

impurities and soaked in sterile distilled deionized water (SDDW) at room temperature (RT) for 24 h. The leaves were then air-dried at RT for 24 h and ground into a powder, stored at 4°C until used. The powder (8 g) was mixed with 150 ml SDDW and stirred at 60°C for 1 h. The extract was then cooled, filtered, and centrifuged at 5,000 rpm for 20 min to obtain the leaf extract.

Green synthesis of ZnO MPs

ZnO-MPs synthesis process was investigated under various conditions, including the rations of leaf extract and zinc acetate solution ($Zn(CH_3COO)_2$) 0.01 M; temperature and reaction time. After the reaction, the mixture was centrifuged at 5,000 rpm for 20 min. MPs were then washed several times with SDDW, dried at 60 ℃ for 24 h, and weighed the amount of products. The synthesis condition, which the greatest amount of ZnO MPs gained, was chosen to apply for further experiments.

Design of the response surface method

The effects of three independent variables ($Zn(CH_3COO)_2$ 0.01 M, temperature, and reaction time) were examined using the RSM method (Design Expert v13, USA). The ranges of the independent variables were set based on the results of wet lab experiments. According to previously published works considering the Optimal Custom design, this optimization under RSM was also applied in this study (Salahi et al., 2023; Subramani et al., 2020).

Characterization of ZnO MPs

UV-visible spectrophotometry (UV-Vis) was performed using Vis Jasco V730 spectrophotometer. Fourier transform infrared spectroscopy (FT-IR) analysis was carried out based on the KBr disks method using Jasco FT/IR-4600 instrument. Dynamic Light Scattering (DLS) analysis was performed using a Horiba SZ-100 nanoparticle size analyzer. Scanning electron microscopic (SEM) analysis and Energy-dispersive X-ray spectroscopy (EDX) were conducted using Hitachi FESEM S4800 and EDX-8100 instruments, respectively.

Seed Germination assay

The seed germination assay was performed following a previous study with several modifications (Sánchez-Pérez et al., 2023). The *V. radiata* seeds were washed with 70% ethanol for 1-2 min, followed by immediately rewashing with distilled water. The seeds were then soaked under 5% sodium hypochlorite solution for 30 min before rinsing with distilled water at least three times. This assay was then conducted as follows: 50 seeds were placed in each box and kept at RT for 8 hours of light - 16 hours of darkness cycles for 14 days. The boxes were sprayed daily with or without 5 mL ZnO-MPs solution at the concentration of 0, 50, 75, and 100 mg/L and 5 mL $K_2Cr_2O_7$ solution [Cr(VI)] of 5 mM. The control treatment was applied with the same volume of distilled water. The number of germinated seeds was counted at 5, 10, and 14 day intervals, and the germination percentage (GP%), germination index (GI), and mean germination time (MGT) were calculated according to the following equation:

$$GP = \frac{\text{Number of germination seeds}}{\text{Total number of seeds}} \times 100 \text{ (eq.1)}$$

$$GI = \Sigma(Gt/Tt); \qquad MGT = \frac{\Sigma[(G_t - G_{t-i}) \times Tt]}{GP} \text{ (eq. 2)}$$

Where **Gt** is the germination percentage at day Tt; **Gt-i** is the germination percentage at the observed time before Tt; **Tt** is the observed time (Li et al., 2021; Sarkhosh et al., 2022).

Seedling assay

The seedling assay was carried out as in previous studies with some modifications (Li et al., 2021; Sarkhosh et al., 2022). In brief, *V. radiata* sterilized seeds were placed at RT with 8 hours of light - 16 hours of darkness cycles for two days for germination. After that, the seeds containing the embryo were randomly selected for the following steps: (i) prepare the seedling pots with 130 g coconut coir; (ii) 15 embryo seeds were randomly selected and sowed into the pots; (iii) sprayed daily with or without of 10 mL ZnO-MPs solution at the concentration of 0, 50, 75, and 100 mg/L and 10 mL of 5 mM $K_2Cr_2O_7$ solution. Distilled water was used as the negative control. After 10 days, the plants were harvested, and several morphological indicators of plants were observed, including stem length (SL), root length (RL), and fresh weight (FW).

Potassium permanganate reduction assay

The potassium permanganate reduction (PPR) assay was performed according to the previous report with some modifications (Kasote et al., 2019). In brief, the fresh solution $KMnO_4$ at a concentration of 80

mg/mL was prepared using the phosphate buffer pH 9.0. The 2 mL of this $KMnO_4$ solution was added to each well, which contained the *V. radiata* leaves (0.1 g) or 1 mL of tannic acid solution at a concentration of 0.5 mg/mL as a positive control. The mixtures were incubated in the dark at RT for 30 min. The absorbance of the mixtures was measured at 525 nm using the UV-Vis reader (UV Vis Jasco V730). The percentage of PPR activity was calculated by comparing the absorbance of the samples to the negative control.

ABTS radical cation decolorization assay

ABTS radical cation decolorization assay was performed according to the previous report with some modifications (Kasote et al., 2019). In brief, the ABTS solution was prepared from an equal volume of aqueous 7.0 mM ABTS and 2.45 mM $K_2S_2O_8$ solutions and kept overnight in the dark. 2 mL of this ABTS solution was then added to each well which contained the *V. radiata* leaves (0.1 g) or 1 mL of tannic acid solution at concentration 0.5 mg/mL as a positive control. The mixtures were incubated in the dark at RT for 30 min. After removing the leaves, the absorbance of the mixtures was measured at 730 nm using the UV-Vis reader (UV Vis Jasco V730). The percentage of ABTS radical cation decolorization activity was evaluated by comparing the absorbance of the samples to the negative control.

Statistical analysis

Statistically significant *p* values were established at $p < 0.05$ in three different experiments, which were conducted using analysis of variance (ANOVA) in the Minitab software.

Results

Synthesis of ZnO MPs

Three factors were chosen to investigate suitable conditions for synthesizing the ZnO MPs, including volume ratio of $Zn(CH_3COO)_2$ 0.01 M: leaf extract, temperature, and reaction time. To understand the role of the volume ratio of $Zn(CH_3COO)_2$ 0.01 M: leaf extract in ZnO MPs production, the volume ratio was tested from 95:5 to 5:95 at temperature 70°C and a reaction time of 60 min. As shown in Table 1, the greatest amount of ZnO MPs were obtained when the reaction condition of volume ratio was 55:45. Based on this result, the following reactions were set up with the fixed volume ratio parameter (55:45) while temperature and reaction time were designed as the changed parameters. After optimizing these conditions, the most efficient temperature and time reaction were suggested at 70°C and 60 min, respectively (Table 1). Taken together, the parameters of volume ratio, temperature, and reaction time at 55:45, 70°C, and 60 min, respectively, were applied to synthesize ZnO MPs on a large scale.

This study observed the wet lab experimental and theoretical results through the RSM method and proposed suitable conditions for large-scale synthesis. As presented in Fig. 1A and Table S1, the RSM model was suggested as a quadratic equation (eq.3). This equation could become a potential predictive model to estimate product quantity (mg) following three independent factors (A, $Zn(CH_3COO)_2$ 0.01 M; B, temperature; and C, reaction time).

Table-1. Effects of volume ratio of $Zn(CH_3COO)_2$ 0.01 M : leaf extract; temperature and reaction time on the synthesis of ZnO MPs products

	$Zn(CH_3COO)_2$ + leaf extract (10 mL)					Temperature		
No.	**Ratio**	**ZnO MPs (mg)**	**No.**	**Ratio**	**ZnO MPs (mg)**	**No.**	**T(°C)**	**ZnO MPs (mg)**
1	95:5	0.0 ± 0.0000^{h}	11	45:55	3.5 ± 0.3606^{abc}	1	50	2.5 ± 0.2^{c}
2	90:10	1.1 ± 0.4359^{g}	12	40:60	3.7 ± 0.2000^{ab}	2	60	3.2 ± 0.1155^{b}
3	85:15	2.6 ± 0.1528^{cde}	13	35:65	3.4 ± 0.2887^{abc}	3	**70**	**3.9 ± 0.2050^{a}**
4	80:20	2.9 ± 0.2517^{bcd}	14	30:70	3.4 ± 0.4359^{abc}	4	80	2.1 ± 0.2646^{c}
5	75:25	2.9 ± 0.1732^{bcd}	15	25:75	3.2 ± 0.3606^{abcd}	**Reaction time**		
6	70:30	3.1 ± 0.1732^{abcd}	16	20:80	2.4 ± 0.2646^{def}	**No.**	**Time (min)**	**ZnO MPs (mg)**
7	65:35	3.2 ± 0.3055^{abcd}	17	15:85	1.7 ± 0.3786^{fg}	1	30	1.6 ± 0.2082^{b}
8	60:40	3.2 ± 0.1732^{abcd}	18	10:90	1.9 ± 0.4163^{efg}	2	**60**	**3.9 ± 0.3055^{a}**
9	**55:45**	**3.9 ± 0.2000^{a}**	19	5:95	1.4 ± 0.1732^{g}	3	90	3.8 ± 0.0577^{a}
10	50:50	3.6 ± 0.2887^{ab}				4	120	3.6 ± 0.2517^{a}

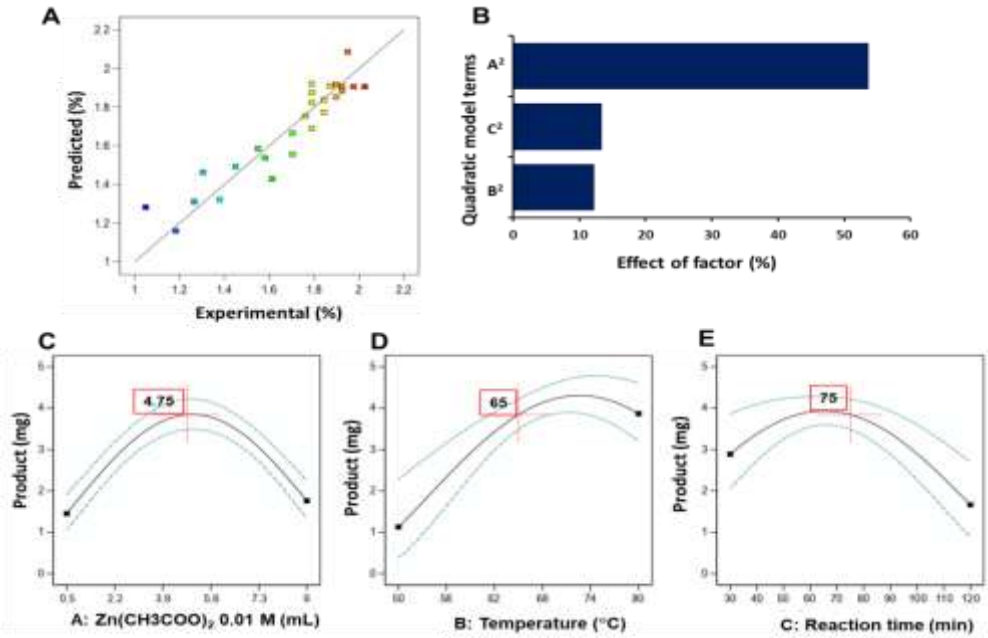

Figure-1. **(A) The RSM model's predicted versus experimental SQRT(product); (B) Pareto analysis showing the contribution of major terms to the product amount response; (C-E) The individual effects of different variables ($Zn(CH_3COO)_2$ 0.01 M, temperature, and reaction time) on the product amount.**

Table-2. Effect of ZnO MPs on seed germination under Cr(VI) stress

Group	GP (%)	Tt (day)	Gt (%)	GI (%)	MGT (day)
Control	96	5	92	34.46	5.38
		10	92		
		14	96		
Cr(VI)	46	5	32	14.29	6.52
		10	46		
		14	46		
Cr(VI) + ZnO 50 mg/L	64	5	62	23.37	5.16
		10	64		
		14	64		
Cr(VI) + ZnO 75 mg/L	70	5	70	26	5.00
		10	70		
		14	70		
Cr(VI) + ZnO 100 mg/L	82	5	78	29.66	5.24
		10	82		
		14	82		
ZnO 50 mg/L	94	5	84	32.51	5.70
		10	90		
		14	94		
ZnO 75 mg/L	88	5	80	31.09	5.45
		10	88		
		14	88		
ZnO 100 mg/L	92	5	86	32.97	5.33
		10	92		
		14	92		

$$SQRT(product) = 0.3804A + 0.1303B - 0.1074C + 0.0021BC - 0.0385A^2 - 0.0020B^2 - 0.0002C^2 \quad \text{(eq.3)}$$

Two of the 26 predicted runs with different variable combinations had residual values less than 0.01 when compared to their actual SQRT(product) values (Fig. 1A and Table S1). Other runs had residuals from -0.2330 to 0.1837. These results demonstrated that the reduced quadratic model was strongly linked with these factors. The ANOVA (Table S2) also showed that the p-values of the statistical significance of the model and all terms were above the 99% confidence level. To ensure model confidence, the lack of fit *p*-value (0.1732, non-significant), R^2 (0.9969), and adjusted R^2 (0.9958) indicated an appropriate fit to experimental data. For distinguishing signal and noise, the adequate precision value was 16.1673, higher than the desirable value of 4.0, demonstrating the established robustness in the RSM model (Bezerra et al., 2008; Mäkelä, 2017).

Three parameters' effects were examined using RSM one-factor plots and 3D surface plots. Fig. 1B indicated that $Zn(CH_3COO)_2$ 0.01 M (A) had the greatest impact on product yield, whereas temperature (B) and reaction time (C) had less. Figs. 1C-E indicate that the optimal conditions for high product yield were $Zn(CH_3COO)_2$ 0.01 M (4.75 mL ~ volume ratio 4.75:5.25), 65°C temperature, and 75

min reaction time. The product mean value is estimated as 3.84 mg (95% prediction intervals: 2.92-4.87 mg). Compared to the expected product amount (3.64 mg) at 55:45, 70°C, and 60 min, the experimental product amount (3.9 mg) was within the 95% prediction interval (2.77−4.61 mg). These results showed that the RSM model matched computational and experimental design requirements. For the interactive and combined effects of the factors, 3D product surface plots were created. The predicted ranges for $Zn(CH_3COO)_2$ 0.01 M (3.5−6.3 mL volume ratio from 3.5:6.5 to 6.3:3.7), temperature (66.3−78.9°C), and reaction time (61−69 min) with a high product value of 3.9−4.3 mg are shown in Fig. 2. Nevertheless, when using 3D surface plots on large scales, the standard error should be considered.

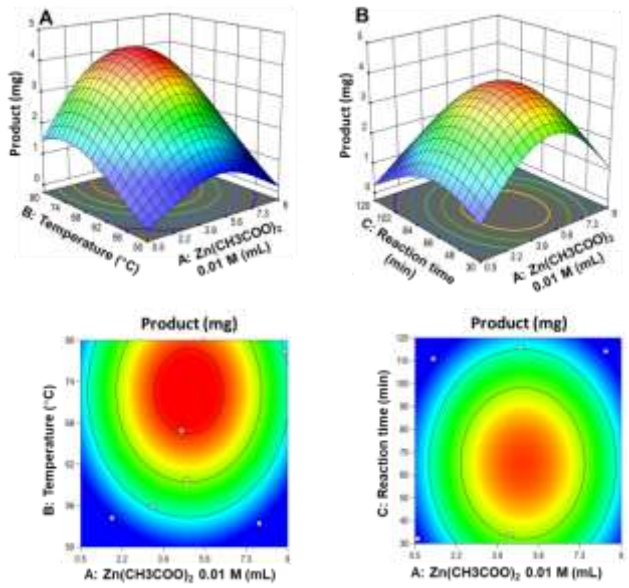

Figure-2. The 3D surface plots showing the interaction effects of $Zn(CH_3COO)_2$ 0.01 M, and temperature (A), $Zn(CH_3COO)_2$ 0.01 M and reaction time (B) on the product amount response.

Characterization of ZnO MPs

The ZnO particles were obtained in different colors (including white, brown, and black) depending on the component of the plant extract and the synthesis method. In previous studies using a calcination step, ZnO particles were typically obtained in white color because the high temperature (400-500°C) of this step could remove all organic components binding on the surface of products (Abdelbaky et al., 2022; Karam and Abdulrahman, 2022). Without the calcination step in this study, the ZnO MPs were recorded in brown color. The results suggested that the synthesis process without calcination maintains the organic compounds from the leaf extract on ZnO MPs and keeps the benefit of leaf extract when applied to the ZnO MPs on plants, such as providing nutrients and enhancing sustainable development.

The surface morphology of ZnO MPs was determined by FE-SEM analysis. The morphology of ZnO MPs varied from small nonspherical particles to big polyhedral nanoparticles with some agglomeration in cluster form (Fig. 3A). In addition, the DLS analysis was applied to clarify the particle size of ZnO MPs. Data illustrated in Fig. 3B indicated that the particle size distribution of ZnO MPs was 1.64 ± 0.56 µm. These results revealed that the ZnO products were synthesized in microparticle sizes according to our simple procedures.

The UV-Vis spectrum was utilized for verifying the formation of ZnO MPs from the reaction between $Zn(CH_3COO)_2$ and the aqueous leaf extract. The $Zn(CH_3COO)_2$ 0.01 M solution did not show any peak from 250 to 600 nm. In contrast, the maximum absorption peak of the aqueous leaf extract and ZnO MPs were obtained at 310 and 290 nm, respectively (Fig. 3C). Compared with previous studies (Naiel et al., 2022; Rajendran et al., 2021), the UV-Vis spectrum of ZnO NPs typically displayed the absorption peak at 350-370 nm, but ZnO MPs was synthesized in this study showed the absorption peak at 290 nm. This result indicated that ZnO MPs products were significantly different from ZnO NPs from other reports.

FT-IR of ZnO MPs was measured from 400-4,000 cm^{-1} range. As shown in Fig. 3D and Fig. S1, the band of $Zn(CH_3COO)_2$ at 1558 and 1444 cm^{-1} related to the existence of the C=O group, while the band at 3115 cm^{-1} and 1017, 953 cm^{-1} could be associated with the stretching of –OH, and C-O linkage, respectively (spectrum I). The bands at 3379, 1613, 1517, 1412, and 1075 cm^{-1} represented the characteristic absorption of the stretching of –OH, C=O groups, and C-O linkage contained in the organic compounds of leaf extract, respectively (spectrum II). The FT-IR analysis of ZnO MPs (spectrum III) showing no absorption band at 1558, 1444, and 953 cm^{-1} demonstrated that the CH_3COO- group was no longer bound into the surface of ZnO MPs; the appearance of a strong band at 1060 cm^{-1} also indicated the existence of C-O linkage

containing in the organic compounds of leaf extract.

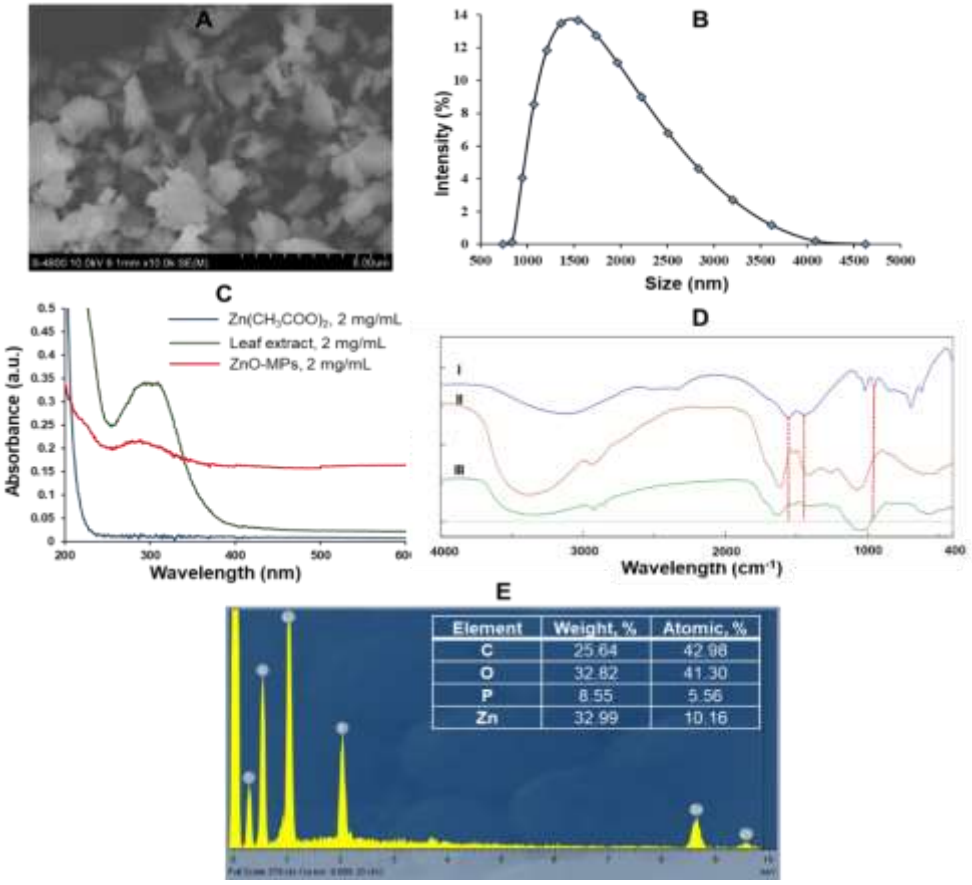

Figure-3. Determined the characterization of ZnO MPs using different techniques, including (A) FE-SEM; (B) DLS analysis; (C) UV-Vis; (D) FT-IR spectra of $Zn(CH_3COO)_2$ (spectrum I), the leaf extract of *D. spathacea* (spectrum II), ZnO MPs (spectrum III); (E) EDX analysis of ZnO MPs.

Besides that, bands at 2917, 2849, and 557 cm^{-1} related to the characteristic absorption of the Zn-O bond without affecting other functional groups from leaf extract (Jayarambabu et al., 2015). According to these results, the synthesis process has successfully created ZnO MP products by binding organic compounds into the MP surface. To determine the elemental component of ZnO MPs, EDX analysis was carried out. The MPs content Zn and O with weight % values of 32.99 and 32.82%, respectively (Fig. 3E). The remaining 34.19% of weight % value was considered to other elements, including C and P. These results strongly suggested that ZnO MPs contained ZnO and organic compounds of aqueous leaf extract.

Effect of ZnO MPs on seed germination under Cr(VI) stress

Various concentrations of ZnO MPs (0, 50, 75, and 100 mg/ L) were used to investigate the effect of ZnO-MPs on the germination of seeds exposed with or without Cr(VI). The Gt of seeds was calculated on days 5, 10, and 14. Under Cr(VI) stress, GP and Gt of seeds significantly decreased compared to those unexposed with Cr(VI) (Table 2). The seeds exposed to Cr(VI) and ZnO MPs at various concentrations (50, 75, and 100 mg/L) recorded GP and Gt rising from 64% to 82% compared to the Cr(VI) exposed seeds at 46%. The effect of ZnO MPs on seed germination without Cr stress was also evaluated. ZnO MPs at different concentrations (50, 75, and 100 mg/L) did not change the Gt and GP of seeds at the statistical levels compared with the control group. Overall, after 14 days of germination, the GI of the Cr(VI) stress group displayed the lowest values at 14.29% of others, while MGT showed the highest value at 6.52 days of other groups. According to these data, the study strongly suggested that ZnO MPs could protect the seeds against the Cr(VI) stress through the absorption of Cr(VI) into the MPs

without any effect on the seed germination process.

Table-3. Effect of ZnO-MPs 100 mg/L on the root/stem length and fresh weight of *V. radiata* under Cr stress condition.

No.	Group	RL (cm)	SL (cm)	Total FW (mg)
1	Control	11.17± 1.026[a]	23.93± 0.351[a]	271.30± 14.50[a]
2	Cr(VI)	4.10± 0.872[c]	13.20± 0.656[c]	113.30± 12.06[c]
3	Cr(VI) + ZnO 100 mg/L	6.70± 0.600[b]	19.83± 0.737[b]	206.00± 9.00[b]
4	ZnO 100 mg/L	9.60± 1.044[a]	23.57± 0.208[a]	272.00± 9.07[a]

Different letters (a, b, and c) presented the statistical results using the Tukey test ($p < 0.05$).
RL: root length; SL: stem length; FW: fresh weight.

Effect of ZnO MPs on *V. radiata* growth under Cr(VI) stress

To screen the effect of ZnO-MPs on plant growth, the root length (RL), stem length (SL), and fresh weight (FW) under Cr(VI) stress, the seedling experiment was observed. As shown in Fig. 4A and Table S3, RL, SL, and FW significantly changed under Cr(VI) stress in comparison with the control group. Contrariwise, the phenotypes and biomass of the plant significantly increased when applied with ZnO MPs at different concentrations under Cr stress. Based on the above screening results, the effect of ZnO-MPs 100 mg/L on *V. radiata* growth under Cr(VI) stress was performed in three independent experiments. The exposure of Cr(VI) significantly reduced the RL, SL, and FW values compared to the control group (Table 3). These values raised with the supplementation of ZnO-MPs at approximately 6.70 cm, 19.83 cm, and 206.00 mg compared to the Cr(VI) stress group, about 4.10 cm, 12.20 cm, and 113.30 mg, respectively. In addition, the result in Table 3 strongly clarified that RL, SL, and FW values of ZnO-MPs exposure alone were no statistically significant difference compared to control group values.

Effect of ZnO MPs on the antioxidant capacity of *V. radiata* leaves under Cr(VI) stress

In plants, antioxidants play an essential role in preventing oxidative processes. Therefore, in this study, the antioxidant capacity of non-enzymatic antioxidants was evaluated using ABTS radical cation decolorization and $KMnO_4$ reduction methods. As shown in Fig. 4B, the scavenging activities using ABTS and $KMnO_4$ methods of non-enzymatic antioxidants from leaves under Cr(VI) stress significantly diminished (46.83 ± 1.938% and 69.60 ± 2.17%, respectively) as compared to the control group (64.47 ± 4.207% and 82.57 ± 1.47%, respectively). Interestingly, the supplement of ZnO-MPs increased the scavenging activities (55.44 ± 2.624% and 78.07 ± 0.820%, respectively) for the Cr(VI) stress seedling group. The application of ZnO-MPs alone unchanged these activities compared to the control group.

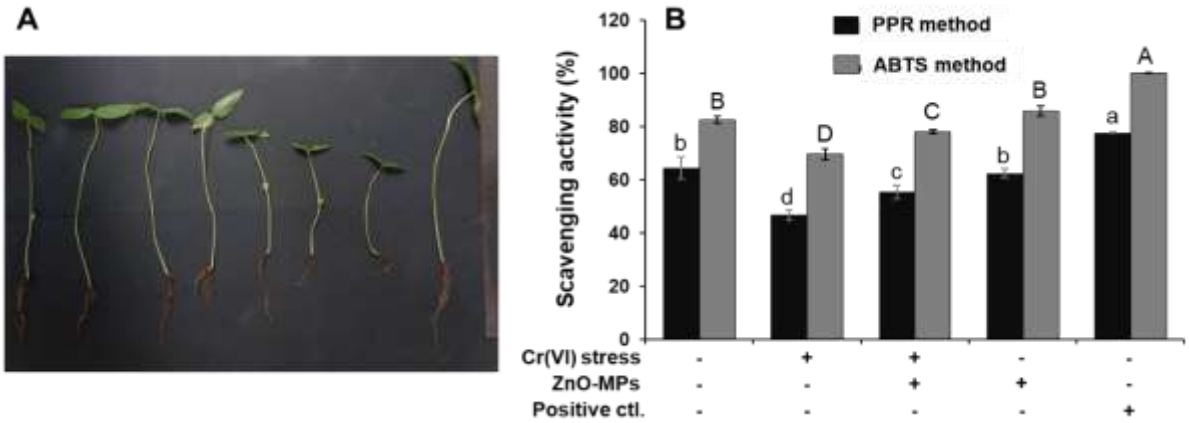

Figure-4. (A) Effect of ZnO MPs on the morphology of *V. radiata* under Cr(VI) stress. From left to right, the symbols of plants were the following: control; Cr(VI) only, Cr(VI) + ZnO-MPs at different concentrations of 50, 75, and 100 mg/L; ZnO-MPs at various concentrations of 50, 75, and 100 mg/L. (B) Effect of ZnO MPs on the antioxidant capacity of *V. radiata* leaves under Cr stress. Tannic acid was used as a positive control. Different letters (a, b, c, d) and (A, B, C, D) presented the statistical results for the PPR and ABTS methods, respectively, using the Tukey test ($p < 0.05$).

Discussion

Cr(VI) contamination in food chain systems causes many diseases when accumulated in living things, such as malignancy, acute vomiting, and diarrhea, (Ali et al., 2023). It is necessary to suggest safe and sustainable ways to decrease toxic Cr(VI) in soil transferring to food crops without affecting crop yield. Recently, the application of nanotechnology and microtechnology in the agriculture field has focused on enhancing the resistance of plants against heavy metals as well as reducing the accumulation of these metals in different plant parts (Basit et al., 2022; Faizan et al., 2021). Previous reports indicated that nanomaterials, such as ZnO-NPs, could be used as surface adsorbents to reduce the accumulation of metals in plants, as well as nutrients and agents to enhance gene metabolism (Basit et al., 2022; Prakash et al., 2022). Nevertheless, the common synthesis methods of ZnO-NPs required a muffle furnace to carry out the unsustainable calcination step for farmers. Therefore, the primary objective of this study was to propose a simple, inexpensive, nontoxic, and sustainable energy method for ZnO-MPs synthesis. Another main purpose of this study is to investigate whether the ZnO-MPs ameliorated Cr(VI) stress in legume plants (*V. radiata*).

Green synthesis of brown color ZnO-MPs was achieved by the reaction between $Zn(CH_3COO)_2$ solution and the aqueous leaf extract of *D. spathacea*. According to previous studies, the formation of ZnO particles is usually recorded with a white color because the calcination step removed all organic components binding on the surface of products (Abdelbaky et al., 2022; Karam and Abdulrahman, 2022). On the contrary, without the calcination step, the ZnO MPs were obtained at brown color, and organic compounds from the leaf extract were still bound on ZnO MPs and maintained the advantages of leaf extract on MPs. Based on the FE-SEM and DLS results, the surface morphology of ZnO particles had small nonspherical particles to big polyhedral nanoparticles with some agglomeration in cluster form and particle sizes of 1.64 ± 0.56 µm. It suggested that these products were synthesized in microparticle sizes. The ZnO-MPs products were also confirmed using other methods, such as UV-Vis, FT-IR spectra, and EDX analysis.

In comparison with previous studies (Naiel et al., 2022; Rajendran et al., 2021), ZnO MPs possess significantly different characteristics from ZnO NPs. Nanosized particles had higher transport in the leaf interior through stomata than microparticle sizes (Eichert et al., 2008; Hua et al., 2022; Kumar et al., 2021). In 2021, Rajput et al. reported that ZnO-NPs with particle size < 50 nm could induce toxic effects on the physiological and anatomical indices of *Hordeum sativum* L. and the Zn accumulation in plant tissues derived from ZnO NPs caused damage to the structural organization of the photosynthetic apparatus and reduced the photosynthetic activities (Rajput et al., 2021). Jingli D. also suggested the phosphorus fertilizer application could reduce the rice uptake of excessive Zn under Zn-contaminated soil (Ding et al., 2021). Interestingly, in this study, ZnO MPs products containing elemental P (8.55% weight, Fig. 2) proposed the molecular mechanism of P–Zn interactions. This phosphorus elemental could contribute to decreasing the plant uptake of excessive Zn. Taken together, this study successfully synthesized ZnO MPs to prevent the Zn accumulation in plants that originated from ZnO NPs, but it still ensures that ZnO MPs-treated plants could protect them against the Cr(VI) toxins.

In the plant-growing process, seed germination plays a vital role in crop yield. This study suggested that the GP, Gt, and GI values of Cr-stress seeds significantly decreased compared to those unexposed with Cr(VI), while the Cr-stress seeds treated with ZnO MPs recorded GP, Gt, and GI values raising comparison to the Cr(VI) exposed seeds only. Our finding matched several previous reports about the role of ZnO particles in enhancing seed germination under heavy metal stress (Basit et al., 2022; Prakash et al., 2022). In addition, the seeds treated with ZnO MPs alone did not change the GP, Gt, and GI values compared to the control group. These results evidenced that microsized particles could enter more difficultly into seed coat pores than nanoparticles, leading to non-enhancing of the activities of starch-degrading and antioxidant enzymes, which increased germination traits (Basit et al., 2022; Itroutwar et al., 2020).

Antioxidants have an essential role in preventing the oxidative processes of plants by counteracting free radicals such as reactive oxygen species (ROS) and reactive nitrogen species (RNS),...(Bunaciu et al., 2012) Antioxidants could be classified based on their structures, including enzymatic antioxidants [ascorbate peroxidase (APX), catalase (CAT), glutathione peroxidase (GPX), glutathione reductase (GR), glutathione transferase (GST), superoxide

dismutase (SOD)] or non-enzymatic antioxidants (polyphenols, vitamins, carotenoids,…). Several antioxidant enzyme genes of plants could be reduced under Cr(VI) stress, and the expression of these genes was significantly upregulated during the addition of ZnO particles (Basit et al., 2022; Prakash et al., 2022). Therefore, in this study, the expression of antioxidant enzyme genes of enzymatic antioxidants from *V. radiata* leaves under Cr(VI) stress was not measured again; instead, the antioxidant capacity of non-enzymatic antioxidants was evaluated. Our results showed that the Cr(VI)-stress plants significantly reduced the RL, SL, FW, and antioxidant capacity of non-enzymatic antioxidants compared to the control group. However, these values increased during the Cr-stress plants treated with ZnO-MPs. Besides, RL, SL, FW, and antioxidant capacity of non-enzymatic antioxidants of plants treated with ZnO-MPs alone were no statistically significant difference compared to control group values. These phenotypic visualizations proved that ZnO-MPs could enter less into the plant system through stomata, root hairs, or leaf surfaces. The present work further strengthened studies about ZnO-MPs to absorb other heavy metals in the environment that pose risks to both human health and ecological systems with effective and safe aspects to low-income populations of the tropics.

Conclusion

During the screening processes for green synthesis conditions of ZnO MPs from $Zn(CH_3COO)_2$ solution and aqueous leaf extract of *D. spathacea*, the successful and reproducible method was based on computational and experimental designs. ZnO MPs were characterized by surface morphology, particle sizes, and elemental components using modern techniques (DLS, EDX, FT-IR, SEM, and UV-Vis). The application of ZnO MPs to protect the legume plant (*V. radiata*) against the Cr(VI) stress during seed germination and seedling vigor of *V. radiata* was successfully evaluated. The results demonstrated that ZnO MPs could enhance the seed germination stage, plant growth, and antioxidative activities under Cr(VI) stress. Moreover, it was suggested that ZnO MPs could enter less into the plant system or seed coat pores than nanoparticles, leading to decreased Zn accumulation in plants that originated from ZnO MPs. This study is an essential report for the agricultural field and provides new strategies to develop the eco-friendly green zinc-micronutrient fertilizer that reduces heavy metal contamination of crops.

Acknowledgment

We express our sincere thanks to the College of Natural Sciences, Can Tho University, for facility support.

Disclaimer: None.
Conflict of Interest: None.
Source of Funding: None.

Contribution of Authors

Pham-Khanh NH: Designed research methodology, experimentation, data analysis and wrote & edited original draft of the article
Ha TKQ: Designed research methodology, performed theoretical calculation & formal analysis, reviewed & edited the article and supervised the study.
NQ Huynh and HNB Le: Performed experiments and reviewed & edited the article

References

Abdelbaky AS, Abd El-Mageed TA, Babalghith AO, Selim S and Mohamed AMHA, 2022. Green synthesis and characterization of ZnO nanoparticles using *Pelargonium odoratissimum* (L.) aqueous leaf extract and their antioxidant, antibacterial and anti-inflammatory activities. Antioxidants. 11(8): 1444. https://doi.org/10.3390/antiox11081444.

Ali S, Mir RA, Tyagi A, Manzar N, Kashyap AS, Mushtaq M, Raina A, Park S, Sharma S and Mir ZA, 2023. Chromium toxicity in plants: signaling, mitigation, and future perspectives. Plants. 12(7): 1502. https://doi.org/10.3390/plants12071502.

Arshad M, Khan AHA, Hussain I, Anees M, Iqbal M, Soja G, Linde C and Yousaf S, 2017. The reduction of chromium (VI) phytotoxicity and phytoavailability to wheat (*Triticum aestivum* L.) using biochar and bacteria. Appl. Soil Ecol. 114: 90–98. https://doi.org/10.1016/j.apsoil.2017.02.021.

Basit F, Nazir MM, Shahid M, Abbas S, Javed MT, Naqqash T, Liu Y and Yajing G, 2022.

Application of zinc oxide nanoparticles immobilizes the chromium uptake in rice plants by regulating the physiological, biochemical and cellular attributes. Physiol. Mol. Biol. Plants. 28: 1175–1190. https://doi.org/10.1007/s12298-022-01207-2.

Bezerra MA, Santelli RE, Oliveira EP, Villar LS and Escaleira LA, 2008. Response surface methodology (RSM) as a tool for optimization in analytical chemistry. Talanta. 76: 965–977. https://doi.org/10.1016/j.talanta.2008.05.019.

Bunaciu AA, Aboul-Enein HY and Fleschin S, 2012. FTIR spectrophotometric methods used for antioxidant activity assay in medicinal plants. Appl. Spectrosc. Rev. 47: 245–255. https://doi.org/10.1080/05704928.2011.645260.

Cheung KH and Gu JD, 2007. Mechanism of hexavalent chromium detoxification by microorganisms and bioremediation application potential: a review. Int. Biodeterior. Biodegradation. 59: 8–15. https://doi.org/10.1016/j.ibiod.2006.05.002.

Choppala G, Bolan N and Park JH, 2013. Chromium contamination and its risk management in complex environmental settings. Adv. Agron. 120: 129–172. https://doi.org/10.1016/B978-0-12-407686-0.00002-6.

Ding J, Liu L, Wang C, Shi L, Xu F and Cai H, 2021. High level of zinc triggers phosphorus starvation by inhibiting root-to-shoot translocation and preferential distribution of phosphorus in rice plants. Environ. Pollut. 277: 116778. https://doi.org/10.1016/j.envpol.2021.116778.

Eichert T, Kurtz A, Steiner U and Goldbach HE, 2008. Size exclusion limits and lateral heterogeneity of the stomatal foliar uptake pathway for aqueous solutes and water-suspended nanoparticles. Physiol. Plant. 134: 151–160. https://doi.org/10.1111/j.1399-3054.2008.01135.x.

Faizan M, Bhat JA, Hessini K, Yu F and Ahmad P, 2021. Zinc oxide nanoparticles alleviates the adverse effects of cadmium stress on *Oryza sativa* via modulation of the photosynthesis and antioxidant defense system. Ecotoxicol. Environ. Saf. 220: 112401. https://doi.org/10.1016/j.ecoenv.2021.112401.

Hauschild MZ, 1993. Putrescine (1, 4-diaminobutane) as an indicator of pollution-induced stress in higher plants: barley and rape stressed with Cr (III) or Cr (VI). Ecotoxicol. Environ. Saf. 26: 228–247. https://doi.org/10.1006/eesa.1993.1052.

Hua Z, Ma S, Ouyang Z, Liu P, Qiang H and Guo X, 2022. The review of nanoplastics in plants: Detection, analysis, uptake, migration and risk. TrAC Trends Anal. Chem. 158: 116889. https://doi.org/10.1016/j.trac.2022.116889.

Itroutwar PD, Govindaraju K, Tamilselvan S, Kannan M, Raja K and Subramanian KS, 2020. Seaweed-based biogenic ZnO nanoparticles for improving agro-morphological characteristics of rice (*Oryza sativa* L.). J. Plant Growth Regul. 39: 717–728. https://doi.org/10.1007/s00344-019-10012-3.

Jayarambabu N, Kumari BS, Rao KV and Prabhu YT, 2015. Beneficial role of zinc oxide nanoparticles on green crop production. Int. J. Multidiscip. Adv. Res. Trends. 2: 273–282.

Jin SE and Jin HE, 2021. Antimicrobial activity of zinc oxide nano/microparticles and their combinations against pathogenic microorganisms for biomedical applications: from physicochemical characteristics toc pharmacological aspects. nanomaterials. 11: 263. https://doi.org/10.3390/nano11020263.

Karam ST and Abdulrahman AF, 2022. Green synthesis and characterization of ZnO nanoparticles by using thyme plant leaf extract. Photonics. 9(8): 594. https://doi.org/10.3390/photonics9080594.

Karimi-Maleh H, Ayati A, Ghanbari S, Orooji Y, Tanhaei B, Karimi F, Alizadeh M, Rouhi J, Fu L and Sillanpää M, 2021. Recent advances in removal techniques of Cr (VI) toxic ion from aqueous solution: A comprehensive review. J. Mol. Liq. 329: 115062. https://doi.org/10.1016/j.molliq.2020.115062.

Kasote DM, Jayaprakasha GK and Patil BS, 2019. Leaf disc assays for rapid measurement of antioxidant activity. Sci. Rep. 9: 1884. https://doi.org/10.1038/s41598-018-38036-x.

Kim SK, Nair RM, Lee J and Lee SH, 2015. Genomic resources in mungbean for future breeding programs. Front. Plant Sci. 6: 626. https://doi.org/10.3389/fpls.2015.00626.

Kumar Y, Tiwari KN, Singh T and Raliya R, 2021. Nanofertilizers and their role in sustainable agriculture. Ann. Plant Soil Res. 23, 238–255. https://doi.org/10.47815/apsr.2021.10067.

Li Y, Liang L, Li W, Ashraf U, Ma L, Tang X, Pan S, Tian H and Mo Z, 2021. ZnO nanoparticle-

based seed priming modulates early growth and enhances physio-biochemical and metabolic profiles of fragrant rice against cadmium toxicity. J. Nanobiotechnology. 19: 1–19. https://doi.org/10.1186/s12951-021-00820-9.

Mäkelä M, 2017. Experimental design and response surface methodology in energy applications: A tutorial review. Energy Convers. Manag. 151: 630–640. https://doi.org/10.1016/j.enconman.2017.09.021.

Naiel B, Fawzy M, Halmy MWA and Mahmoud AED, 2022. Green synthesis of zinc oxide nanoparticles using Sea Lavender (*Limonium pruinosum* L. Chaz.) extract: Characterization, evaluation of anti-skin cancer, antimicrobial and antioxidant potentials. Sci. Rep. 12: 20370. https://doi.org/10.1038/s41598-022-24805-2.

Nair RM, Pandey AK, War AR, Hanumantharao B, Shwe T, Alam A, Pratap A, Malik SR, Karimi R and Mbeyagala EK, 2019. Biotic and abiotic constraints in mungbean production—progress in genetic improvement. Front. Plant Sci. 10: 1340. https://doi.org/10.3389/fpls.2019.01340.

Nguyen PD, Abedini A, Gangloff SC and Lavaud C, 2018. Antimicrobial constituents from leaves of *Dolichandrone spathacea* and their relevance to traditional use. Planta Medica Int. Open. 5: 14–23. https://doi.org/10.1055/s-0043-125339.

Prakash V, Rai P, Sharma NC, Singh VP, Tripathi DK, Sharma S and Sahi S, 2022. Application of zinc oxide nanoparticles as fertilizer boosts growth in rice plant and alleviates chromium stress by regulating genes involved in oxidative stress. Chemosphere. 303: 134554. https://doi.org/10.1016/j.chemosphere.2022.134554.

Rajendran NK, George BP, Houreld NN and Abrahamse H, 2021. Synthesis of zinc oxide nanoparticles using Rubus fairholmianus root extract and their activity against pathogenic bacteria. Molecules. 26: 3029. https://doi.org/10.3390/molecules26103029.

Rajput VD, Minkina T, Fedorenko A, Chernikova N, Hassan T, Mandzhieva S, Sushkova S, Lysenko V, Soldatov MA and Burachevskaya M, 2021. Effects of zinc oxide nanoparticles on physiological and anatomical indices in spring barley tissues. Nanomaterials. 11: 1722. https://doi.org/10.3390/nano11071722.

Ramzan M, Naz G, Parveen M, Jamil M, Gill S and Sharif HMA, 2023. Synthesis of phytostabilized zinc oxide nanoparticles and their effects on physiological and anti-oxidative responses of *Zea mays* (L.) under chromium stress. Plant Physiol. Biochem. 196: 130–138. https://doi.org/10.1016/j.plaphy.2023.01.015.

Rani S, Kumari N and Sharma V, 2023. Biosynthesized zinc oxide nanoparticles as a novel nanofertilizer influence growth, yield, antioxidant enzymes, and arsenic accumulation in Mungbean (*Vigna radiata* L.) under arsenic stress. J. Soil Sci. Plant Nutr. 23: 2360–2380. https://doi.org/10.1007/s42729-023-01188-5.

Saffari R, Shariatinia Z and Jourshabani M, 2020. Synthesis and photocatalytic degradation activities of phosphorus containing ZnO microparticles under visible light irradiation for water treatment applications. Environ. Pollut. 259: 113902. https://doi.org/10.1016/j.envpol.2019.113902.

Salahi F, Zarei-Jelyani F, Farsi M and Rahimpour MR, 2023. Optimization of hydrogen production by steam methane reforming over Y-promoted Ni/Al_2O_3 catalyst using response surface methodology. J. Energy Inst. 108: 101208. https://doi.org/10.1016/j.joei.2023.101208.

Sánchez-Pérez DM, Flores-Loyola E, Márquez-Guerrero SY, Galindo-Guzman M and Marszalek JE, 2023. Green synthesis and characterization of zinc oxide nanoparticles using larrea tridentata extract and their impact on the *in-vitro* germination and seedling growth of *Capsicum annuum*. Sustainability. 15: 3080. https://doi.org/10.3390/su15043080.

Sarkhosh S, Kahrizi D, Darvishi E, Tourang M, Haghighi-Mood S, Vahedi P and Ercisli S, 2022. Effect of zinc oxide nanoparticles (ZnO-NPs) on seed germination characteristics in two Brassicaceae family species: *Camelina sativa* and *Brassica napus* L. J. Nanomater. 2022: 1–15. https://doi.org/10.1155/2022/1892759.

Singh D, Sharma NL, Singh CK, Yerramilli V, Narayan R, Sarkar SK and Singh I, 2021. Chromium (VI)-induced alterations in physio-chemical parameters, yield, and yield characteristics in two cultivars of mungbean (*Vigna radiata* L.). Front. Plant Sci. 12: 735129. https://doi.org/10.3389/fpls.2021.735129.

Subramani S, Govindasamy R and Rao GLN, 2020. Predictive correlations for NOx and smoke emission of DI CI engine fuelled with diesel-biodiesel-higher alcohol blends-response surface

methodology approach. Fuel. 269: 117304. https://doi.org/10.1016/j.fuel.2020.117304.

Sun J, Yang Z and Teng L, 2020. Nanotechnology and microtechnology in drug delivery systems. Dose-Response. 18(2). https://doi.org/10.1177/1559325820907810.

Thao TTP, Chi NL, Luu NT, Dung NT, Van-Loc T, Van-Tuan N, Hung TQ and Nhung NTA, 2021. Phytochemistry and anti-inflammatory activity of iridoids from *Dolichandrone spathacea* collected in the mangrove forest of Phu Loc district, Thua Thien Hue province, Vietnam. Vietnam J. Chem. 59: 943–950. https://doi.org/10.1002/vjch.202100121.